Mechanism and site of action of big dynorphin on ASIC1a

Borg, C.B.; Braun, N.; Heusser, S.A.; Bay, Y.; Weis, D.; Galleano, I.; ... ; Pless, S.A.

Mechanism and site of action of big dynorphin on ASIC1a

Christian B. Borg[a,1], Nina Braun[a,1], Stephanie A. Heusser[a], Yasmin Bay[a], Daniel Weis[a], Iacopo Galleano[a], Camilla Lund[a], Weihua Tian[b,c], Linda M. Haugaard-Kedström[a], Eric P. Bennett[b,c], Timothy Lynagh[a], Kristian Strømgaard[a], Jacob Andersen[d], and Stephan A. Pless[a,2]

[a]Department of Drug Design and Pharmacology, University of Copenhagen, 2100 Copenhagen, Denmark; [b]Copenhagen Center for Glycomics, Department of Cellular and Molecular Medicine, University of Copenhagen, 2200 Copenhagen, Denmark; [c]Copenhagen Center for Glycomics, Department of Odontology, University of Copenhagen, 2200 Copenhagen, Denmark; and [d]Department of Molecular Biology, Vipergen ApS, 1610 Copenhagen, Denmark

Edited by Richard W. Aldrich, The University of Texas at Austin, Austin, TX, and approved February 13, 2020 (received for review November 6, 2019)

Acid-sensing ion channels (ASICs) are proton-gated cation channels that contribute to neurotransmission, as well as initiation of pain and neuronal death following ischemic stroke. As such, there is a great interest in understanding the in vivo regulation of ASICs, especially by endogenous neuropeptides that potently modulate ASICs. The most potent endogenous ASIC modulator known to date is the opioid neuropeptide big dynorphin (BigDyn). BigDyn is up-regulated in chronic pain and increases ASIC-mediated neuronal death during acidosis. Understanding the mechanism and site of action of BigDyn on ASICs could thus enable the rational design of compounds potentially useful in the treatment of pain and ischemic stroke. To this end, we employ a combination of electrophysiology, voltage-clamp fluorometry, synthetic BigDyn analogs, and noncanonical amino acid-mediated photocrosslinking. We demonstrate that BigDyn binding results in an ASIC1a closed resting conformation that is distinct from open and desensitized states induced by protons. Using alanine-substituted BigDyn analogs, we find that the BigDyn modulation of ASIC1a is primarily mediated through electrostatic interactions of basic amino acids in the BigDyn N terminus. Furthermore, neutralizing acidic amino acids in the ASIC1a extracellular domain reduces BigDyn effects, suggesting a binding site at the acidic pocket. This is confirmed by photocrosslinking using the noncanonical amino acid azidophenylalanine. Overall, our data define the mechanism of how BigDyn modulates ASIC1a, identify the acidic pocket as the binding site for BigDyn, and thus highlight this cavity as an important site for the development of ASIC-targeting therapeutics.

ligand–receptor interaction | neuropeptide | acid-sensing ion channel | noncanonical amino acids | voltage-clamp fluorometry

Neuropeptides are a diverse class of signaling molecules that are involved in a wide variety of physiological functions, including the modulation of neurotransmission (1, 2). The neuropeptide subclass of dynorphins is best known for its modulation of the G protein-coupled opioid receptors (3–5), through which they mediate spinal analgesia. However, it is increasingly recognized that these highly basic peptides also modulate the activity of ionotropic receptors, such as tetrameric glutamate receptors (*N*-methyl-D-aspartate subtype) and trimeric acid-sensing ion channels (ASICs) (6–10). The latter interaction is of particular interest, as ASICs have emerged as mediators of both pain and stroke and thus represent potential targets in the treatment of these diseases (11–17). In fact, big dynorphin (BigDyn) is the most potent endogenous ASIC modulator described to date. The neuropeptide was found to rescue proton-gated currents after exposure to steady-state desensitization-inducing conditions in homomeric ASIC1a and heteromeric ASIC1a/2a and ASIC1a/2b channels in the nanomolar range and thereby promote acidosis-induced neuronal cell death in cultured neurons (10, 18). As ASIC1a homomers and ASIC1a-containing heteromers are the most prevalent isoforms in the nervous system, this raises the possibility that inhibitors or competitors of the ASIC1a–BigDyn interaction might prove valuable therapeutics. However, despite this potential therapeutic relevance, the underlying mechanism behind this potent modulation remains elusive.

BigDyn (32 aa) and its two smaller peptide fragments, dynorphin A (DynA, 17 aa) and dynorphin B (DynB, 13 aa), are cleavage products of the prodynorphin precursor peptide (4, 5, 19). Genes encoding BigDyn are broadly conserved among vertebrates. Both BigDyn and DynA display nanomolar affinities for a range of related opioid receptors (4). BigDyn was reported to be ∼1,000-fold more potent in its modulation of ASIC1a steady-state desensitization compared to DynA, while DynB did not modulate ASIC1a steady-state desensitization (10). This raises the possibility of a unique ASIC-selective pharmacophore.

Here, we set out to investigate the molecular determinants of the high-potency modulation of ASIC1a by BigDyn and identify the binding site on ASIC1a. Interestingly, previous data on the well-studied ASIC1a-modulator spider toxin psalmotoxin-1 (PcTx1), which increases the apparent proton sensitivity and consequently enhances steady-state desensitization (20), pointed toward a possible role of the ASIC1a acidic pocket in BigDyn modulation: first, preincubation in PcTx1 has been shown to prevent BigDyn modulation of ASIC1a, suggesting that the two peptides might compete for an overlapping binding site (10). Second, the positively charged toxin is bound at the acidic pocket

Significance

Neuropeptides such as big dynorphin (BigDyn) play important roles in the slow modulation of fast neurotransmission, which is mediated by membrane-embedded receptors. In fact, BigDyn is the most potent known endogenous modulator of one such receptor, the acid-sensing ion channel (ASIC), but the mode of action remains unknown. In this work, we employ a broad array of technologies to unravel the details of where big dynorphin binds to ASIC and how it modulates its activity. As both BigDyn and ASIC are implicated in pain pathways, this work might pave the way toward future analgesics.

Author contributions: C.B.B., N.B., S.A.H., L.M.H.-K., E.P.B., T.L., K.S., J.A., and S.A.P. designed research; C.B.B., N.B., S.A.H., Y.B., D.W., I.G., C.L., W.T., and L.M.H.-K. performed research; I.G., W.T., and E.P.B. contributed new reagents/analytic tools; C.B.B., N.B., S.A.H., Y.B., D.W., I.G., C.L., L.M.H.-K., and E.P.B. analyzed data; and C.B.B., N.B., S.A.H., and S.A.P. wrote the paper.

The authors declare no competing interest.

This article is a PNAS Direct Submission.

Data deposition: DNA sequences and data related to electrophysiological and fluorometry recordings are freely available on Zenodo (DOI: 10.5281/zenodo.3686253).

[1]C.B.B. and N.B. contributed equally to this work.

[2]To whom correspondence may be addressed. Email: stephan.pless@sund.ku.dk.

This article contains supporting information online at https://www.pnas.org/lookup/suppl/doi:10.1073/pnas.1919323117/-/DCSupplemental.

First published March 12, 2020.

in ASIC1a–PcTx1 X-ray cocrystal structures (21, 22), again raising the possibility of a similar binding site for BigDyn, which carries a net charge of +9.

In order to directly probe the molecular determinants of the high-potency modulation of ASIC1a by BigDyn, we employ a multiangle strategy: we introduce complementary charge-neutralizing mutations in ASIC1a, as well as BigDyn, and study their functional consequences on channel modulation in electrophysiology experiments. We further use voltage-clamp fluorometry (VCF) recordings to monitor the conformational changes resulting from the ASIC1a–BigDyn interaction. Finally, the noncanonical amino acid photocrosslinker azidophenylalanine (AzF) (23, 24) is incorporated at the acidic pocket of ASIC1a to covalently cross-link ASIC–BigDyn complexes using ultraviolet (UV) light exposure. Together, our results demonstrate that BigDyn binds at the acidic pocket through charge–charge interactions and reduces the proton sensitivity of both activation and steady-state desensitization of ASIC1a, likely by inducing a distinct closed state of the channel.

Results

BigDyn Affects pH Dependence of mASIC1a and Induces a Unique Closed State. First, we set out to test the ability of BigDyn and its proteolytic products (Fig. 1*A*) to rescue proton-gated currents after exposure to steady-state desensitization-inducing conditions of wild-type (WT) mouse ASIC1a (mASIC1a) using two-electrode voltage-clamp (TEVC) electrophysiology. Steady-state desensitization was induced using conditioning in pH 7.1, which decreased subsequent pH 5.6-induced current response to 5.7% (95% confidence interval [95CI]: 3.8, 7.6%) compared to that after conditioning in pH 7.4 ("control"). However, application of 1 μM BigDyn during the pH 7.1 conditioning step largely rescued pH 5.6-induced currents, resulting in 90.1% (95CI: 77.9, 102.3%) of the control current response. The half-maximal effective concentration (EC_{50}) for this current rescue was 210.6 nM (95CI: 162.6, 258.6 nM) BigDyn; *SI Appendix*, Fig. S1 *A* and *B*). By contrast, applying DynA and DynB during conditioning did not produce significant current rescue when applied at a concentration of 1 μM (at pH 7.1) (Fig. 1 *B* and *C*), although at a concentration of 3 μM, DynA partially rescued pH 5.6-induced current (*SI Appendix*, Fig. S1*C*). Furthermore, coapplication of 1 μM DynA or Dyn1-19 (containing the Arg18 and Lys19 that link DynA and DynB in full-length BigDyn) with DynB during conditioning did not reproduce the phenotype observed with full-length BigDyn (Fig. 1 *B* and *C*). Next, we sought to assess if the presence of BigDyn would affect the pH dependence of activation or steady-state desensitization in WT mASIC1a. Indeed, even the presence of a subsaturating BigDyn concentration (0.1 μM) resulted in a small right-shift in the pH_{50} of activation (from 6.80 [95CI: 6.70, 6.91] to 6.66 [95CI: 6.61, 6.70], $P = 0.0172$) and of steady-state desensitization (from 7.21 [95CI: 7.19, 7.24] to 7.15 [95CI: 7.12, 7.19], $P = 0.0225$) (Fig. 1*D* and *SI Appendix*, Table S1).

The above results suggested that the potency of both proton activation and steady-state desensitization was lowered in the presence of BigDyn, but it remained unclear if this occurred through a stabilization of the canonical resting closed state (relative to open/steady-state desensitized states) or if BigDyn induced a distinct protein conformation. To distinguish between these possibilities, we turned to VCF, which allows us to directly probe ion

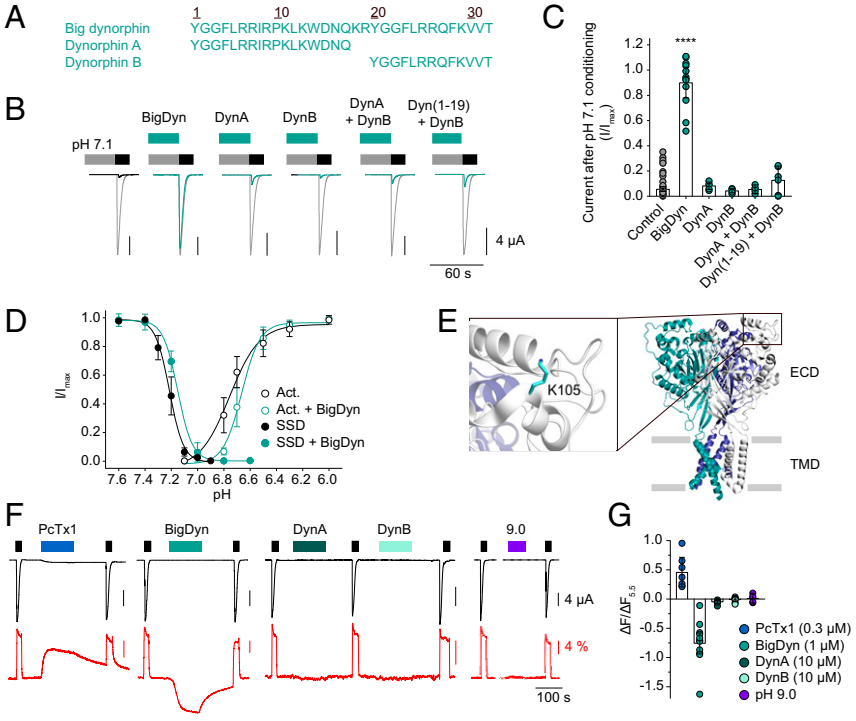

Fig. 1. Mechanism of ASIC1a modulation by BigDyn. (*A*) Amino acid sequences of BigDyn, DynA, and DynB. (*B* and *C*) Representative current traces (*B*) and averaged data (*C*) obtained by pH 5.6 application (black bar in *B*) at mASIC1a WT-expressing *Xenopus laevis* oocytes after preincubation in pH 7.1 (gray bar) with or without 1 μM of the indicated peptide or peptide combination (green bar); in *B*, control currents (after pH 7.4 conditioning) are shown in gray for comparison. Asterisks indicate significant difference to control condition ($P < 0.0001$); $n = 5$–68). (*D*) Concentration-response curves for activation (Act.) and steady-state desensitization (SSD) of WT ASIC1a in the presence and absence of 0.1 μM BigDyn ($n = 4$–15). (*E*) Structure of the ECD and transmembrane domain (TMD) of cASIC1 (PDB: 4NTW) with individual subunits color coded and *Inset* showing the location of Lys105. (*F*) Representative current (black) and fluorescence (red) traces obtained by application of pH 5.5 (black bars) at mASIC1a labeled with Alexa Fluor 488 at position 105, the indicated peptide (PcTx1, 0.3 μM: blue bar; BigDyn, 1 μM: green bar; DynA, 10 μM: dark green bar; and DynB, 10 μM: light green bar) or pH 9.0 (purple bar). (*G*) Averaged change in fluorescence obtained by application of PcTx1, BigDyn, DynB, or pH 9.0, as shown in *F* (normalized to that obtained by application of pH 5.5) ($n = 5$–15). Error bars in *C*, *D*, and *G* represent 95CI.

channel conformational rearrangements using environmentally sensitive fluorescent dyes (25). In agreement with earlier reports (26), Alexa Fluor 488-labeled Lys105Cys mutants (Fig. 1*E*) showed robust and reversible pH-induced current and fluorescence changes (Fig. 1*F* and *SI Appendix*, Table S2). The upward deflection of the fluorescence signal is likely associated with channel desensitization, as the pH response curve of the fluorescence closely matches that of steady-state desensitization (*SI Appendix*, Fig. S2*A* and Table S3). Additionally, application of 0.3 μM tarantula toxin PcTx1, reported to stabilize the desensitized state of ASIC1a by increasing the proton sensitivity (20, 27) through binding to the acidic pocket (21, 22), also induces an upward deflection in fluorescence (dequenching) without inducing current (Fig. 1 *F* and *G*). By contrast, application of 1 μM BigDyn did not result in a current response, but caused a downward deflection (quenching) of the fluorescence signal, in stark contrast to the upward deflection observed with increased proton concentrations and PcTx1. This quenching is dependent on the BigDyn concentration, with a half-maximal effect in the high nanomolar range (*SI Appendix*, Fig. S2*B*), slightly higher than what was observed for its functional EC_{50} on the WT channel (850 nM [95CI: 299, 1402 nM] and 211 nM [95CI: 163, 259 nM], respectively). Importantly, no fluorescence change was observed upon application of 10 μM DynA or 10 μM DynB or increasing the pH to 9.0 (Fig. 1 *F* and *G* and *SI Appendix*, Table S2), demonstrating that the BigDyn-induced conformation is dependent on a functionally active peptide and distinct from that elicited by low (or high) pH. Together, the data show that mASIC1a modulation by BigDyn is dependent on a continuous peptide sequence containing at least parts of both DynA and DynB and indicates that BigDyn might be stabilizing a closed resting conformation of ASIC1a that is distinct from that induced by protons and PcTx1.

Contribution of Positively Charged BigDyn Side Chains to Modulation of ASIC1a. An unusual feature of BigDyn is its high density of positive charge (net charge +9, Fig. 2*A*). We therefore reasoned that the interaction with ASIC1a might be driven by electrostatic forces, i.e., by binding to negatively charged side chains on ASIC1a. To investigate the contribution of individual positively charged amino acids (Arg and Lys) of BigDyn to its ability to modulate ASIC1a steady-state desensitization, we generated BigDyn analogs with individual positively charged residues substituted for alanine (Ala). These 10 BigDyn Ala-analogs were tested for their ability to rescue current at WT mASIC1a when applied at 1 μM at a conditioning pH of 7.1 (Fig. 2 *B* and *C*). Indeed, individual alanine substitutions of the three most N-terminally located positively charged amino acids (Arg6, Arg7, and Arg9) virtually abolished BigDyn-mediated current rescue: 9.8% (95CI: −2.1, 21.6%) for Arg6Ala, 5.0% (95CI: 1.2, 8.7%) for Arg7Ala, and 2.3% (95CI: 1.7, 3.0%) for Arg9Ala, respectively (*SI Appendix*, Table S4).

By contrast, individual substitution of the remaining positive charges (Lys11, Lys13, Lys18, Arg19, Arg25, Arg26, and Lys29; Fig. 2) or the residue situated between Arg7 and Arg9 (Ile8; *SI Appendix*, Fig. S3*A*) showed less pronounced effects on BigDyn activity (between 29.4 and 76.3% recovery; *SI Appendix*, Table S4). This indicates that the charge of a cluster of three closely positioned Arg in the N-terminal part of BigDyn is important for the functional modulation of mASIC1a, although other properties, such as side chain size and H-bonding ability, might also play a role (Fig. 2). This notion is confirmed by the finding that the EC_{50} for the modulatory effect of the Arg9Ala peptide is increased over 50-fold (Fig. 2*D*). Consistent with the above, substituting the sole negatively charged residue (Asp15) had no effect on its ability to modulate ASIC1a (*SI Appendix*, Fig. S3*A*). Replacing Tyr1, which has been implicated in the activity of BigDyn toward the opioid receptors (19, 28, 29), or Trp14 resulted in a modest, but

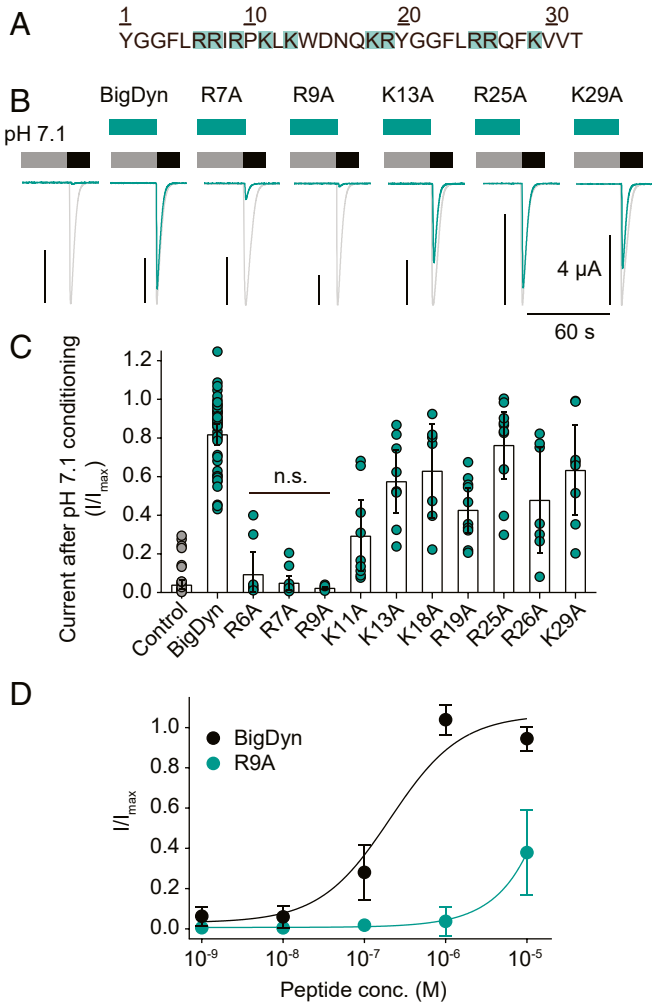

Fig. 2. Positive charges near the BigDyn N terminus are essential for ASIC1a modulation. (*A*) Sequence of BigDyn with basic side chains highlighted in green. (*B* and *C*) Representative current traces (*B*) and averaged data (*C*) obtained by pH 5.6 application (black bar in *B*) at ASIC1a WT-expressing *Xenopus laevis* oocytes after preincubation in pH 7.1 (gray bar) with or without 1 μM of the indicated BigDyn analog (green bar); in *B*, control currents after pH 7.6 conditioning are shown in gray for comparison. (*D*) Concentration-response curves for WT ASIC1a modulation by BigDyn (black) and Arg9Ala (green). Error bars in *C* and *D* represent 95CI. In *C*, n.s. indicates no statistically significant difference to control condition. n = 7–48 in *C*, and n = 7–9 in *D*.

significant decrease in the ability to rescue currents (*SI Appendix*, Fig. S3*A*), while N-terminal truncations generally had more pronounced effects (*SI Appendix*, Fig. S3*B* and Table S5).

Together, the data indicate that the BigDyn-mediated effects on ASIC1a are primarily driven by a cluster of three positively charged side chains in the N-terminal part of the neuropeptide.

Negative Charges within the Acidic Pocket Are Crucial for BigDyn Modulation of ASIC1a. To complement our findings with BigDyn, we next wanted to identify its binding site on ASIC1a. As we found the basic charge of BigDyn to be a crucial determinant of the interaction, we set out to mutate negatively charged side chains in the mASIC1a extracellular domain (ECD). Specifically, we focused our attention on a cavity in the ASIC1a ECD denoted the acidic pocket, which contains a high density of negatively charged residues (30). The acidic pocket also serves as the binding site of PcTx1 (21, 22, 31), which has been suggested

to compete with BigDyn for ASIC1a modulation (10). We introduced charge-neutralizing amino acid substitutions to individual acidic side chains (Asp to Asn and Glu to Gln substitutions) at eight positions in and around the acidic pocket (Fig. 3*A*). As ASIC1a mutations, especially around the acidic pocket, often lead to a change in pH sensitivity, the pH dependence of steady-state desensitization for each of the mutant mASIC1a constructs was determined in order to identify the appropriate steady-state desensitization conditioning pH for each mutant (*SI Appendix*, Fig. S4 and Table S6). Next, we tested the mASIC1a variants for their sensitivity toward 1 μM BigDyn, applied during steady-state desensitization conditioning. However, all tested single mutants retained significant pH 5.6-induced current rescue (Fig. 3 *B* and *C* and *SI Appendix*, Table S7), indicating that single charge-neutralizing amino acid substitutions in or near the acidic pocket alone are not enough to abolish the effect of BigDyn.

We therefore sought to investigate whether combined mutation of two acidic residues in the acidic pocket would abolish BigDyn modulation. Four acidic residues are found in close proximity on the upper thumb and finger domains (Asp237, Glu238, Asp345, and Asp349; Fig. 3*A*) and have been suggested to interact as two carboxyl–carboxylate pairs (Asp237–Asp349 and Glu238–Asp345) (30). We therefore generated mASIC1a variants carrying a combination of two charge-neutralizing Asp to Asn and/or Glu to Gln mutations of these four residues and measured their pH dependence of steady-state desensitization (*SI Appendix*, Fig. S4 and Table S6). The double mutant mASIC1a constructs were then tested for their sensitivity to BigDyn modulation using the same protocol as for the single mutations, except that Asp237Asn/Asp345Asn was activated at pH 4.0 in order to reach saturating currents. All four tested acidic pocket double mutants showed a drastically decreased sensitivity to 1 μM BigDyn compared to WT mASIC1a (Fig. 3 *B* and *C* and *SI Appendix*, Table S7). The biggest decrease in rescue of pH 5.6-induced currents was observed for Glu238Gln/Asp345Asn ASIC1a. For this construct, application of 1 μM BigDyn during steady-state desensitization conditioning resulted in 6.8% (95CI: 1.7, 11.8%) current compared to pH 5.6-induced currents after pH 7.6 conditioning, which was comparable to the control response observed in absence of BigDyn (Fig. 3 *B* and *C*). Additionally, the Glu238Gln/Asp345Asn double mutant showed a roughly 50-fold increase in the EC_{50} for the modulatory effect of BigDyn (Fig. 3*D*). As the Hill slope of ASIC1a steady-state desensitization is unusually steep, we sought to confirm that the loss of the BigDyn effect observed for the double mutants was not due to a shift in pH sensitivity that rendered the channels overall unresponsive. As detailed in *SI Appendix*, Fig. S5*A* and Table S7, this was not the case, although the Asp237Asn/Asp349Asn mutant showed a moderately reduced effect when a different conditioning pH was employed. Additionally, we combined the Glu238Gln/Asp345Asn double mutant with the Lys105Cys mutation (used for VCF experiments) resulting in a variant that showed robust pH-induced

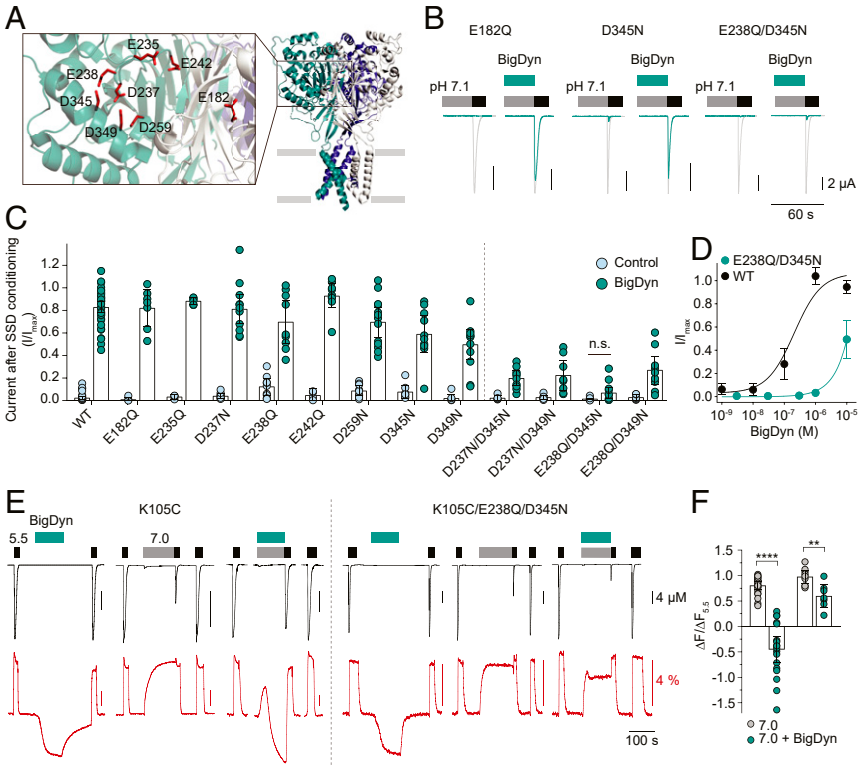

Fig. 3. Double charge-neutralizing mutations around the ASIC1a acidic pocket reduce BigDyn modulation. (*A*) Structure of cASIC1 (PDB: 4NTW) with individual subunits color coded and *Inset* showing the location of acidic side chains mutated to Gln or Asn. (*B* and *C*) Representative current traces (*B*) and averaged data (*C*) obtained by pH 5.6 application (black bar in *B*) after preincubation in SSD-inducing pH (gray bar; see *SI Appendix*, Fig. S4 and Table S6 for details) with or without (control) 1 μM BigDyn (green bar) at *Xenopus laevis* oocytes expressing the indicated ASIC1a construct; in *B*, control currents after pH 7.6 conditioning are shown in gray for comparison (n = 4–45). n.s. indicates no statistically significant difference to control condition. (*D*) Concentration-response curves for BigDyn-mediated modulation of WT (black) and Glu238Gln/Asp345Asn mutant (green) ASIC1a (n= 7–9). (*E*) Representative current (black) and fluorescence (red) traces from channels labeled with Alexa Fluor 488 at position 105 obtained by application of pH 5.5 (black bar), 7.0 (gray bar) or 1 μM BigDyn (green bar) at mASIC1a Lys105Cys (*Left*) and Lys105Cys/Glu238Gln/Asp345Asn (*Right*). (*F*) Averaged change in fluorescence at pH 7.0 with and without 1 μM BigDyn as obtained in *E*, normalized to that obtained by application of pH 5.5; n = 7–22, unpaired t test $^{**}P < 0.01$; $^{****}P < 0.0001$. Error bars in *C*, *D*, and *F* represent 95CI.

fluorescence changes in VCF experiments. Similar to the Glu238Gln/Asp345Asn mutation alone, but contrary to the Lys105Cys single mutant, the Lys105Cys/Glu238Gln/Asp345Asn triple mutant was functionally insensitive to 1 μM BigDyn (Fig. 3*E*, current trace). However, the application of BigDyn at pH 7.6 led to a downward deflection of the fluorescent signal to a similar extent as observed in the Lys105Cys variant (−81.7% [95CI: −27.6–135.9%] and −76.0% [95CI: −58.1, −94.0%]). When conditioning the Lys105Cys variant at pH 7.0 together with BigDyn, we observed a fluorescent signal that likely portrays dequenching due to conformational changes induced by pH 7.0 in the first phase, followed by gradually dominating quenching of the signal as a result of BigDyn binding in the later phase (Fig. 3 *E*, *Left*). The triple mutant, however, presents a distinct fluorescent profile that is dominated by the pH 7.0 upward deflection and no net quenching despite a small BigDyn-dependent reduction in fluorescence intensity (Fig. 3 *E* and *F*). Together, the results indicate that BigDyn still binds to the triple mutant, but with a decreased ability to prevent steady-state desensitization.

Next, we wanted to ascertain that the loss of BigDyn modulation is indeed specific to double charge-neutralizing mutations in or near the acidic pocket. We thus tested two additional double charge-neutralizing mutations at positions outside the acidic pocket, Asp253Asn/Glu245Gln and Glu373Gln/Glu411Gln (*SI Appendix*, Fig. S5 *B* and *C*). Both double mutants retained full sensitivity toward 1 μM BigDyn, indicating that the effect of double charge-neutralizing mutants was specific to the acidic pocket.

In principle, it is possible that the observed loss of current rescue with the double charge-neutralizing mutations in or near the acidic pocket originates from a changed desensitization profile. However, this is highly unlikely, given that there was no correlation between the extent of change in steady-state desensitization and current rescue, and mutants with WT-like or right-shifted steady-state desensitization curves showed a drastic loss of current rescue (e.g., Glu238Gln/Asp345Asn and Glu238Gln/Asp349Asn). Overall, the data therefore strongly imply that the acidic pocket serves as an interaction site for BigDyn.

Photocrosslinking Confirms an Interaction Site in the Acidic Pocket. To further validate the acidic pocket as the BigDyn binding site, we turned to UV-induced photocrosslinking using the photoreactive side chain of the noncanonical amino acid (ncAA) azidophenylalanine (AzF) incorporated at different positions in ASIC1a (Fig. 4 *A* and *B*) (32–34). Incorporating AzF at positions lining the ASIC1a–BigDyn interaction interface should allow covalent trapping of the complex and enable subsequent visualization using Western blotting. To this end, we removed endogenous ASIC1a from human embryonic kidney (HEK) 293T cells by CRISPR/Cas9 (*SI Appendix*, Fig. S6*A*) and expressed human ASIC1a (hASIC1a) variants carrying AzF at Glu177, Thr236, Thr239, Lys343 Glu344, Asp351, Glu355, Lys356, and Asp357, respectively, using the nonsense suppression methodology (Fig. 4 *A* and *B*) (35). Efficient ncAA incorporation was confirmed by comparing the amounts of protein obtained from cells grown in the presence compared to cells grown in the absence of AzF (*SI Appendix*, Fig. S6 *B* and *C*). Notably, while steady-state desensitization of hASIC1a is shifted compared to that of mASIC1a (hASIC1a pH_{50} steady-state desensitization: 7.07 [95CI: 7.03, 7.11] vs. mASIC1a pH_{50} steady-state desensitization 7.24 [95CI: 7.23, 7.25]) (36), the modulatory effect of BigDyn on the human ortholog is virtually identical (*SI Appendix*, Fig. S6 *D*–*F*). As shown in Fig. 4*C*, covalently cross-linked BigDyn was detected in samples containing AzF in and around the acidic pocket only when they were exposed to UV light, but not in control samples processed in absence of UV light or in UV-exposed WT hASIC1a, or when AzF was incorporated in the lower parts of the ECD, i.e., away from the acidic pocket (Phe69, Tyr71, Val80, Asp253, Trp287, Glu413). In summary, incorporation of the ncAA AzF in combination with UV-induced photocrosslinking confirmed that the BigDyn binding site is located at the ASIC1a acidic pocket.

Discussion

Mechanism of Action of BigDyn on ASIC1a. Despite the potential pathophysiological relevance of the ASIC–BigDyn interaction (10), the determinants for the high-potency modulation of ASIC steady-state desensitization by BigDyn have remained enigmatic. A defining characteristic of neuropeptide signaling is its slow time scale relative to the fast transmission achieved by small molecules (1, 2). Indeed, we and others have found that the functional effects of BigDyn on ASIC1a-mediated currents require relatively long preincubation times (ref. 10 and Fig. 1). The notion of a slow binding and unbinding process is directly supported by our VCF data, which demonstrate that the BigDyn-induced conformational changes are concentration-dependent and drastically slower than those induced by changes in proton concentration (Figs. 1 and 3*E* and *SI Appendix*, Fig. S2*B*). Once bound, BigDyn reduces the proton sensitivity of both pH-dependent activation and steady-state desensitization of ASIC1a. Although the acidic pocket is not likely to be the primary proton sensor of ASICs (37, 38), side chains in and around the acidic pocket have been shown to modulate proton sensitivity (30, 37), and X-ray crystallographic data show substantial contraction of this pocket, together with changes in side chain interactions, in low-pH structures (39). A direct binding of BigDyn to this region is therefore expected to alter proton sensing and channel gating in response to protonation. Interestingly, our VCF data suggest that BigDyn binding favors a resting closed state that is distinct from open and desensitized states induced by protons (or PcTx1) (Figs. 1*F* and 3*E*). Although we cannot rule out some degree of direct quenching of the fluorophore by BigDyn, several lines of evidence indicate that the fluorescence change is indeed primarily caused by conformational changes: 1) high concentrations of DynA/B only have neglectable effects on the fluorescent signal, 2) the half-maximal BigDyn concentrations to elicit functional and fluorescence effects are in a similar concentration range, and 3) the BigDyn-insensitive Lys105Cys/Glu238Gln/Asp345Asn triple mutant is only marginally quenched by BigDyn at pH 7.0.

We therefore argue that the BigDyn-induced conformation increases the energetic barrier to populate both open and desensitized states, consistent with the right-shift of both parameters in the presence of BigDyn (Fig. 1). In the case of steady-state desensitization, this would result in ASIC1a remaining responsive to pH drops even under proton concentrations that would normally desensitize the channel, thus explaining the ability of BigDyn to noticeably increase ASIC1a-dependent neuronal death during acidosis (10).

As activation and desensitization both involve the collapse of the acidic pocket, bringing thumb and finger domain Asp side chains from ∼8 Å to within <3 Å of each other (39), we speculate that BigDyn binding hinders the proton-induced transitions from resting closed states to active and/or desensitized states.

Defining the Site of the ASIC1a–BigDyn Interaction. Consistent with the hypothesis that the unusually high density of positive charge of BigDyn is crucial for its functional effects, we find that charge-neutralizing mutations of basic amino acids reduce the ability of BigDyn to rescue ASIC1a proton-gated currents after exposure to steady-state desensitization-inducing conditions. This effect was particularly pronounced for mutations in a cluster of three Arg (Arg6, Arg7, and Arg9) in the N-terminal part of the peptide, while no effect was observed when mutating the only noncharged side chain between amino acids 6 and 9 (Ile8). This is in agreement with the finding that DynA (representing the N-terminal part of BigDyn), but not DynB (representing the C-terminal part of BigDyn), can have modulatory effects on ASICs (10, 40) (*SI Appendix*, Fig. S1*C*). However, it is worth noting that functional effects were also

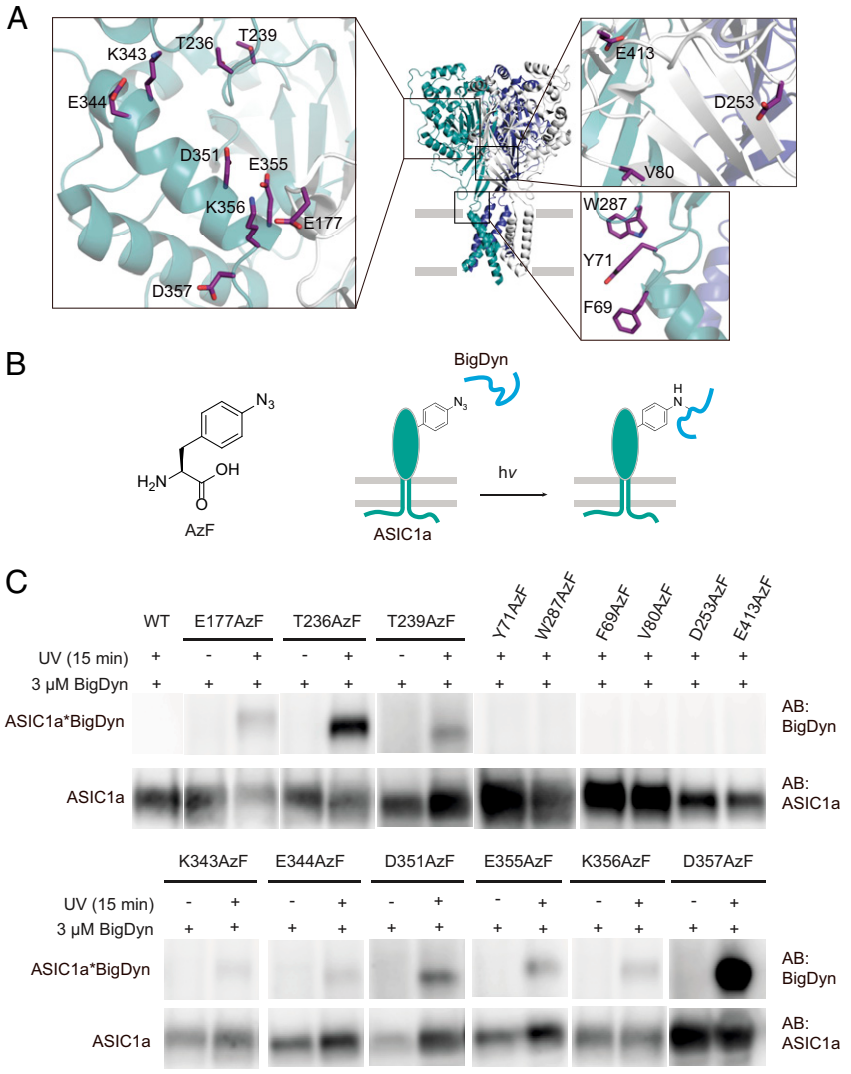

Fig. 4. Photocrosslinking confirms the BigDyn interaction site at the acidic pocket. (*A*) Structure of cASIC1 (PDB: 4NTW) with individual subunits color coded and *Insets* highlighting side chains replaced by 4-Azido-L-phenylalanine (AzF) in the acidic pocket (*Left Inset*) and lower extracellular domain (*Right Insets*). (*B*) Structure of 4-Azido-L-phenylalanine (AzF) and schematic workflow for cross-linking to BigDyn. HEK 293T cells expressing AzF-containing ASIC1a variants are incubated with 3 μM BigDyn and exposed to UV light for 15 min to form covalent ASIC1a–BigDyn complexes. The complex is purified via a C-terminal 1D4 tag on ASIC1a and visualized via Western blotting. (*C*) Western blot of purified hASIC1a WT and variants carrying AzF in the extracellular domain detected using the specified antibodies (AB). BigDyn is detected only in UV-exposed samples containing AzF in the acidic pocket, but absent in control samples not exposed to UV, those carrying AzF in the lower extracellular domain (*Right Insets* in *A*), or WT. See also *SI Appendix*, Fig. S7.

reduced when mutating Lys11, Arg19, Arg26, and Tyr1, albeit to a lesser extent (Fig. 2 and *SI Appendix*, Fig. S3*A*). These data suggest that the interaction of BigDyn with ASIC1a is not solely driven by charge at Arg6, Arg7, and Arg9, but also mediated by other, mostly basic amino acids throughout the peptide sequence. This notion is further supported by data from our N-terminal truncation screen and complemented by the finding that AzF incorporated at positions along the entire length of the cleft formed by the acidic pocket enabled to covalently cross-link to BigDyn. Together, this argues for an extended interaction surface on ASIC1a, likely extending from the peripheral thumb domain around the α5 helix and into the acidic pocket. While the location of the BigDyn binding site is distinct from that suggested for RFamide neuropeptides on ASICs (41, 42), it does overlap with the binding site for PcTx1 (10, 21, 22, 31). This is consistent with the finding that RFamides do not functionally compete with BigDyn or PcTx1 (10, 43). Interestingly, both PcTx1 and BigDyn bind to the acidic pocket through extensive charge–charge interactions, and additional contributions are made by aromatic amino acids [i.e., Trp7 and Trp24 in PcTx1 (31) and Tyr1 in BigDyn]. However, the binding mode is likely to differ substantially between the two peptides, as PcTx1 adopts a rigid fold, while BigDyn is likely unstructured in aqueous solution (44, 45). Indeed, the two peptides have opposite modulatory effects on ASIC1a: while PcTx1 interacts with and stabilizes the desensitized state (27), our data suggest that BigDyn stabilizes a closed/resting state of ASIC1a (see above).

Future studies using computational docking, ligand-binding studies, or a combination of cross-linking and mass spectrometry could further help to provide details on the precise binding mode and orientation of BigDyn at the acidic pocket.

Possible Biological Implications. Intriguingly, both ASIC1a and dynorphins have been shown to exhibit overlapping expression patterns (e.g., amygdala, hippocampus) and to contribute to a similar array of both physiological (learning, memory) and pathophysiological (pain, nociception, addiction) processes (4, 5, 11, 12, 46–52). Among the

dynorphins tested here, BigDyn is the most potent at ASIC1a and has also been shown to greatly enhance acidosis-induced cell death in cortical neurons (10). The potential relevance of this finding is underscored by the fact that under pathophysiological conditions, the BigDyn levels will be sufficient to modulate ASIC activity in vivo (up to low micromolar range) (4, 5, 8, 10, 53, 54). By contrast, the modulatory effects under physiological BigDyn concentrations (1–10 nM) would likely be small, although others have reported a higher sensitivity of ASIC1a toward BigDyn (10). Together, this highlights the potential of the ASIC–BigDyn interaction site as a drug target. Given that BigDyn and PcTx1 share a common binding site, this notion is supported by the finding that PcTx1 or PcTx1-like peptides show promise in limiting neuronal death in stroke models (14, 15). While the ASIC–BigDyn interaction per se increases neuronal death, a therapeutic option might in the future emerge from building upon the scaffold of modified peptides with reduced activity (similar to some presented in this study) that could, if refined, work as silent modulators to prevent the ASIC–BigDyn interaction. Recent work on PcTx1 has shown that peptides targeting the ASIC acidic pocket can display significant functional plasticity. For example, altered pH or mutations within the toxin (Arg27Ala or Phe30Ala) can effectively convert PcTx1 into a potentiator (31, 55). Similarly, and depending on cellular context and presence of cofactors, DynA can act as both an inhibitor and potentiator of glutamate receptors (4). It will thus be intriguing to see if this functional dichotomy is also possible to achieve for BigDyn in order to unlock its potential as an ASIC-targeting therapeutic lead.

Materials and Methods

mASIC1a was expressed in *Xenopus laevis* oocytes, and proton-induced currents were measured with TEVC. Synthetic dynorphin peptides and analogs were tested for their ability to decrease the pH sensitivity and rescue currents of mASIC1a from proton-induced steady-state desensitization (Figs. 1 and 2). Proton- and peptide-induced conformational rearrangements in mASIC1a were monitored by VCF (Fig. 1 *E*–*G*). Site-directed mutagenesis was employed to introduce charge-neutralizing amino acid substitutions of negatively charged residues of the acidic pocket, and the sensitivity of mutant mASIC1a toward BigDyn was assessed by TEVC (Fig. 3). UV cross-linking of BigDyn to hASIC1a was achieved in HEK 293T cells in which endogenous hASIC1a was removed by CRISPR/Cas9 using guide RNA (56). ASIC1a-free HEK 293T cells were transfected with DNA encoding hASIC1a or hASIC1a TAG variants, and AzF was introduced through the nonsense suppression method (35). BigDyn (3 μM) was added to AzF–hASIC1a expressing HEK 293T cells, and the cells were subsequently exposed to UV light for 15 min in order to induce cross-linking. UV-treated cells were lysed, and the UV-induced hASIC1a–BigDyn complex formation was visualized by Western blotting (Fig. 4). See *SI Appendix, Supplementary Text* for detailed description of materials and methods.

Data Availability Statement. Peptides sequences, original Western blots, and more extensive recordings and experimental protocols can be found in the *SI Appendix*. DNA sequences and data related to electrophysiological and fluorometry recordings are freely available on Zenodo (57).

ACKNOWLEDGMENTS. We acknowledge the Lundbeck Foundation (R139-2012-12390 to S.A.P. and R218-2016-1490 to N.B.), the Boehringer Ingelheim Fond (to N.B.), the Danish National Research Foundation (DNRF107 to W.T.), the European Union's Horizon 2020 research and innovation program under the Marie Sklodowska-Curie Grant Agreement 834274 (to S.A.H.), and the University of Copenhagen for financial support.

1. M. P. Nusbaum, D. M. Blitz, E. Marder, Functional consequences of neuropeptide and small-molecule co-transmission. *Nat. Rev. Neurosci.* **18**, 389–403 (2017).
2. A. N. van den Pol, Neuropeptide transmission in brain circuits. *Neuron* **76**, 98–115 (2012).
3. C. Chavkin, I. F. James, A. Goldstein, Dynorphin is a specific endogenous ligand of the kappa opioid receptor. *Science* **215**, 413–415 (1982).
4. K. F. Hauser *et al*., Pathobiology of dynorphins in trauma and disease. *Front. Biosci.* **10**, 216–235 (2005).
5. C. Schwarzer, 30 years of dynorphins—New insights on their functions in neuropsychiatric diseases. *Pharmacol. Ther.* **123**, 353–370 (2009).
6. D. Massardier, P. F. Hunt, A direct non-opiate interaction of dynorphin-(1-13) with the N-methyl-D-aspartate (NMDA) receptor. *Eur. J. Pharmacol.* **170**, 125–126 (1989).
7. L. Chen, Y. Gu, L. Y. Huang, The mechanism of action for the block of NMDA receptor channels by the opioid peptide dynorphin. *J. Neurosci.* **15**, 4602–4611 (1995).
8. L. Chen, Y. Gu, L. Y. Huang, The opioid peptide dynorphin directly blocks NMDA receptor channels in the rat. *J. Physiol.* **482**, 575–581 (1995).
9. S. L. Lai, Y. Gu, L. Y. Huang, Dynorphin uses a non-opioid mechanism to potentiate N-methyl-D-aspartate currents in single rat periaqueductal gray neurons. *Neurosci. Lett.* **247**, 115–118 (1998).
10. T. W. Sherwood, C. C. Askwith, Dynorphin opioid peptides enhance acid-sensing ion channel 1a activity and acidosis-induced neuronal death. *J. Neurosci.* **29**, 14371–14380 (2009).
11. S. Diochot *et al*., Black mamba venom peptides target acid-sensing ion channels to abolish pain. *Nature* **490**, 552–555 (2012).
12. C. J. Bohlen *et al*., A heteromeric Texas coral snake toxin targets acid-sensing ion channels to produce pain. *Nature* **479**, 410–414 (2011).
13. M. Mazzuca *et al*., A tarantula peptide against pain via ASIC1a channels and opioid mechanisms. *Nat. Neurosci.* **10**, 943–945 (2007).
14. Z. G. Xiong *et al*., Neuroprotection in ischemia: Blocking calcium-permeable acid-sensing ion channels. *Cell* **118**, 687–698 (2004).
15. I. R. Chassagnon *et al*., Potent neuroprotection after stroke afforded by a double-knot spider-venom peptide that inhibits acid-sensing ion channel 1a. *Proc. Natl. Acad. Sci. U.S.A.* **114**, 3750–3755 (2017).
16. M. Qiang *et al*., Selection of an ASIC1a-blocking combinatorial antibody that protects cells from ischemic death. *Proc. Natl. Acad. Sci. U.S.A.* **115**, E7469–E7477 (2018).
17. Y. Z. Wang *et al*., Tissue acidosis induces neuronal necroptosis via ASIC1a channel independent of its ionic conduction. *eLife* **4**, e05682 (2015).
18. T. W. Sherwood, K. G. Lee, M. G. Gormley, C. C. Askwith, Heteromeric acid-sensing ion channels (ASICs) composed of ASIC2b and ASIC1a display novel channel properties and contribute to acidosis-induced neuronal death. *J. Neurosci.* **31**, 9723–9734 (2011).
19. S. Podvin, T. Yaksh, V. Hook, The emerging role of spinal dynorphin in chronic pain: A therapeutic perspective. *Annu. Rev. Pharmacol. Toxicol.* **56**, 511–533 (2016).
20. X. Chen, H. Kalbacher, S. Gründer, The tarantula toxin psalmotoxin 1 inhibits acid-sensing ion channel (ASIC) 1a by increasing its apparent H^+ affinity. *J. Gen. Physiol.* **126**, 71–79 (2005).
21. R. J. Dawson *et al*., Structure of the acid-sensing ion channel 1 in complex with the gating modifier Psalmotoxin 1. *Nat. Commun.* **3**, 936 (2012).
22. I. Baconguis, E. Gouaux, Structural plasticity and dynamic selectivity of acid-sensing ion channel-spider toxin complexes. *Nature* **489**, 400–405 (2012).
23. I. Coin *et al*., Genetically encoded chemical probes in cells reveal the binding path of urocortin-I to CRF class B GPCR. *Cell* **155**, 1258–1269 (2013).
24. J. W. Chin *et al*., Addition of p-azido-L-phenylalanine to the genetic code of Escherichia coli. *J. Am. Chem. Soc.* **124**, 9026–9027 (2002).
25. J. Cowgill, B. Chanda, The contribution of voltage clamp fluorometry to the understanding of channel and transporter mechanisms. *J. Gen. Physiol.* **151**, 1163–1172 (2019).
26. G. Bonifacio, C. I. Lelli, S. Kellenberger, Protonation controls ASIC1a activity via coordinated movements in multiple domains. *J. Gen. Physiol.* **143**, 105–118 (2014).
27. X. Chen, H. Kalbacher, S. Gründer, Interaction of acid-sensing ion channel (ASIC) 1 with the tarantula toxin psalmotoxin 1 is state dependent. *J. Gen. Physiol.* **127**, 267–276 (2006).
28. J. M. Walker, H. C. Moises, D. H. Coy, G. Baldrighi, H. Akil, Nonopiate effects of dynorphin and des-Tyr-dynorphin. *Science* **218**, 1136–1138 (1982).
29. M. Wollemann, S. Benyhe, Non-opioid actions of opioid peptides. *Life Sci.* **75**, 257–270 (2004).
30. J. Jasti, H. Furukawa, E. B. Gonzales, E. Gouaux, Structure of acid-sensing ion channel 1 at 1.9 A resolution and low pH. *Nature* **449**, 316–323 (2007).
31. N. J. Saez *et al*., Molecular dynamics and functional studies define a hot spot of crystal contacts essential for PcTx1 inhibition of acid-sensing ion channel 1a. *Br. J. Pharmacol.* **172**, 4985–4995 (2015).
32. S. Ye, T. Huber, R. Vogel, T. P. Sakmar, FTIR analysis of GPCR activation using azido probes. *Nat. Chem. Biol.* **5**, 397–399 (2009).
33. M. H. Poulsen, A. Poshtiban, V. Klippenstein, V. Ghisi, A. J. R. Plested, Gating modules of the AMPA receptor pore domain revealed by unnatural amino acid mutagenesis. *Proc. Natl. Acad. Sci. U.S.A.* **116**, 13358–13367 (2019).
34. H. Rannversson *et al*., Genetically encoded photocrosslinkers locate the high-affinity binding site of antidepressant drugs in the human serotonin transporter. *Nat. Commun.* **7**, 11261 (2016).
35. J. W. Chin, Expanding and reprogramming the genetic code. *Nature* **550**, 53–60 (2017).
36. T. W. Sherwood, C. C. Askwith, Endogenous arginine-phenylalanine-amide-related peptides alter steady-state desensitization of ASIC1a. *J. Biol. Chem.* **283**, 1818–1830 (2008).
37. T. Lynagh, Y. Mikhaleva, J. M. Colding, J. C. Glover, S. A. Pless, Acid-sensing ion channels emerged over 600 Mya and are conserved throughout the deuterostomes. *Proc. Natl. Acad. Sci. U.S.A.* **115**, 8430–8435 (2018).
38. S. Vullo *et al*., Conformational dynamics and role of the acidic pocket in ASIC pH-dependent gating. *Proc. Natl. Acad. Sci. U.S.A.* **114**, 3768–3773 (2017).
39. N. Yoder, C. Yoshioka, E. Gouaux, Gating mechanisms of acid-sensing ion channels. *Nature* **555**, 397–401 (2018).

40. A. Vyvers, A. Schmidt, D. Wiemuth, S. Gründer, Screening of 109 neuropeptides on ASICs reveals no direct agonists and dynorphin A, YFMRFamide and endomorphin-1 as modulators. *Sci. Rep.* **8**, 18000 (2018).
41. M. Reiners *et al*., The conorfamide RPRFa stabilizes the open conformation of acid-sensing ion channel 3 via the nonproton ligand-sensing domain. *Mol. Pharmacol.* **94**, 1114–1124 (2018).
42. B. Bargeton *et al*., Mutations in the palm domain disrupt modulation of acid-sensing ion channel 1a currents by neuropeptides. *Sci. Rep.* **9**, 2599 (2019).
43. M. Salinas *et al*., The receptor site of the spider toxin PcTx1 on the proton-gated cation channel ASIC1a. *J. Physiol.* **570**, 339–354 (2006).
44. G. Ferré, G. Czaplicki, P. Demange, A. Milon, Structure and dynamics of dynorphin peptide and its receptor. *Vitam. Horm.* **111**, 17–47 (2019).
45. C. O'Connor *et al*., NMR structure and dynamics of the agonist dynorphin peptide bound to the human kappa opioid receptor. *Proc. Natl. Acad. Sci. U.S.A.* **112**, 11852–11857 (2015).
46. J. A. Wemmie, R. J. Taugher, C. J. Kreple, Acid-sensing ion channels in pain and disease. *Nat. Rev. Neurosci.* **14**, 461–471 (2013).
47. C. J. Kreple *et al*., Acid-sensing ion channels contribute to synaptic transmission and inhibit cocaine-evoked plasticity. *Nat. Neurosci.* **17**, 1083–1091 (2014).
48. W. Wittmann *et al*., Prodynorphin-derived peptides are critical modulators of anxiety and regulate neurochemistry and corticosterone. *Neuropsychopharmacology* **34**, 775–785 (2009).
49. A. Kuzmin, N. Madjid, L. Terenius, S. O. Ogren, G. Bakalkin, Big dynorphin, a prodynorphin-derived peptide produces NMDA receptor-mediated effects on memory, anxiolytic-like and locomotor behavior in mice. *Neuropsychopharmacology* **31**, 1928–1937 (2006).
50. J. A. Wemmie *et al*., Overexpression of acid-sensing ion channel 1a in transgenic mice increases acquired fear-related behavior. *Proc. Natl. Acad. Sci. U.S.A.* **101**, 3621–3626 (2004).
51. Q. Wang *et al*., Fear extinction requires ASIC1a-dependent regulation of hippocampal-prefrontal correlates. *Sci. Adv.* **4**, eaau3075 (2018).
52. V. I. Pidoplichko *et al*., ASIC1a activation enhances inhibition in the basolateral amygdala and reduces anxiety. *J. Neurosci.* **34**, 3130–3141 (2014).
53. A. Goldstein, V. E. Ghazarossian, Immunoreactive dynorphin in pituitary and brain. *Proc. Natl. Acad. Sci. U.S.A.* **77**, 6207–6210 (1980).
54. B. T. Andrews, T. K. McIntosh, M. F. Gonzales, P. R. Weinstein, A. I. Faden, Levels of endogenous opioids and effects of an opiate antagonist during regional cerebral ischemia in rats. *J. Pharmacol. Exp. Ther.* **247**, 1248–1254 (1988).
55. B. Cristofori-Armstrong, N. J. Saez, I. R. Chassagnon, G. F. King, L. D. Rash, The modulation of acid-sensing ion channel 1 by PcTx1 is pH-, subtype- and species-dependent: Importance of interactions at the channel subunit interface and potential for engineering selective analogues. *Biochem. Pharmacol.* **163**, 381–390 (2019).
56. C. Jin *et al*., Over-expression of ASIC1a promotes proliferation via activation of the β-catenin/LEF-TCF axis and is associated with disease outcome in liver cancer. *Oncotarget* **8**, 25977–25988 (2017).
57. C. B. Borg *et al*., Mechanism and site of action of big dynorphin on ASIC1a [Data set]. Zenodo. http://doi.org/10.5281/zenodo.3686254. Deposited 24 February 2020.